Cancer Letters 465 (2019) 1–11

Contents lists available at ScienceDirect

Cancer Letters

journal homepage: www.elsevier.com/locate/canlet

Original Articles

Concomitant targeting of Hedgehog signaling and MCL-1 synergistically induces cell death in Hedgehog-driven cancer cells

Michael Torsten Meister[a,b,c,d,1], Cathinka Boedicker[a,b,c], Benedikt Linder[e], Donat Kögel[b,e], Thomas Klingebiel[b,c,d], Simone Fulda[a,b,c,*]

[a] Institute for Experimental Cancer Research in Pediatrics, Goethe-University Frankfurt, Komturstr. 3a, 60528, Frankfurt, Germany
[b] German Cancer Consortium (DKTK), Partner Site Frankfurt, Germany
[c] German Cancer Research Center (DKFZ), Heidelberg, Germany
[d] Division of Pediatric Hematology and Oncology, Hospital for Children and Adolescents, Goethe-University, Frankfurt, Germany
[e] Experimental Neurosurgery, Neuroscience Center, Goethe-University Hospital, Frankfurt, Germany

ARTICLE INFO

Keywords:
Rhabdomyosarcoma
Hedgehog signaling
GANT61
A-1210477
MCL-1
NOXA
BIM

ABSTRACT

In the present study, we show that concomitant inhibition of Hedgehog (HH) signaling by the glioma-associated oncogene homolog1 (GLI1)-targeting agent GANT61 and the antiapoptotic BCL-2 protein family member MCL-1 by A-1210477 synergistically induces cell death in HH-driven cancers, i.e. rhabdomyosarcoma (RMS) and medulloblastoma (MB) cells. Combined genetic and pharmacological inhibition emphasized that co-treatment of GANT61 and A-1210477 indeed relies on inhibition of GLI1 (by GANT61) and MCL-1 (by A-1210477). Mechanistic studies revealed that A-1210477 triggers the release of BIM from MCL-1 and its shuttling to BCL-x_L and BCL-2. Indeed, BIM proved to be required for GANT61/A-1210477-induced cell death, as genetic silencing of BIM using siRNA significantly rescues cell death upon GANT61/A-1210477 co-treatment. Similarly, genetic silencing of NOXA results in a significant reduction of GANT61/A-1210477-mediated cell death. Also, overexpression of MCL-1 or BCL-2 significantly protects RMS cells from GANT61/A-1210477-triggered cell death. Addition of the pan-caspase inhibitor zVAD.fmk significantly decreases GANT61/A-1210477-stimulated cell demise, indicating apoptotic cell death. In conclusion, GANT61 and A-1210477 synergize to engage mitochondrial apoptosis. These findings provide the rationale for further evaluation of dual inhibition of HH signaling and MCL-1 in HH-driven cancers.

1. Introduction

RMS, the most common soft-tissue sarcoma in children and adolescents, is the third most frequently occurring solid tumor in this patient cohort [1] and comprises two major histological subtypes: Embryonal RMS (ERMS) predominantly occurs in smaller children, while alveolar RMS (ARMS) primarily affects older children and adolescents. Overall, ERMS shows better prognosis than ARMS which may be attributed to the fact that ARMS more often display metastases upon diagnosis [2,3]. While the cell of origin of different RMS subtypes is still under debate [4], multiple studies on the biological features of RMS cells have already been conducted: While ARMS are characterized by a fusion gene (predominantly PAX3- or PAX7-FOXO1, more infrequently PAX3-NCOA1 or -NCOA2 and others) and infrequent activations of the MYC or CDK4 oncogene [5–7], ERMS commonly harbor a copy-number neutral loss of heterozygosity (LOH) on chromosome 11p [8]. Recent studies employing whole-genome sequencing and other next-generation sequencing techniques suggest a low mutational burden for ARMS, while ERMS typically harbor alterations in the TP53 tumor suppressor gene (including LOH on chromosome 17p13.1, which harbors the TP53 gene, and activating mutations of MDM2, a suppressor of TP53 function) and in RAS signaling (i.e. activating alterations of FGFR4, HRAS, KRAS and NRAS or inactivating alterations of NF1) [9]. Therapeutic regimens for RMS consist of chemotherapy (including compounds such as vincristine, actinomycin-D and ifosfamide), radiation therapy and, if feasible, surgery. Despite major advances made in the field of pediatric tumor therapy in general, patients with RMS still suffer from only mediocre to dismal prognosis, which is especially poor in primary metastatic, refractory or relapsed disease [10].

The HH signaling pathway plays a fundamental role in embryonal

* Corresponding author. Institute for Experimental Cancer Research in Pediatrics, Goethe-University Frankfurt, Komturstr. 3a, Germany.
E-mail address: simone.fulda@kgu.de (S. Fulda).
[1] Current affiliation: Princess Máxima Center for Pediatric Oncology, Utrecht, Netherlands.

https://doi.org/10.1016/j.canlet.2019.08.012
Received 4 July 2019; Received in revised form 21 August 2019; Accepted 23 August 2019
0304-3835/ © 2019 Published by Elsevier B.V.

Abbreviations

ARMS	alveolar RMS
ATCC	American Type Culture Collection
CI	combination index
DSMZ	Deutsche Sammlung von Mikroorganismen und Zellkulturen
ERMS	embryonal RMS
EV	empty vector
FCS	fetal calf serum
FDA	Food & Drug Administration
GLI	glioma-associated oncogene
GLI1	glioma-associated oncogene homolog1
HH	Hedgehog
HPI	Hedgehog pathway inhibitor
IP	immunoprecipitation
JCRB	Japanese Cancer Research Resources Bank
LOH	loss of heterozygosity
MB	medulloblastoma
OE	overexpression
PI	propidium iodide
PTCH	Patched
RMS	rhabdomyosarcoma
SHH	Sonic Hedgehog
SMO	Smoothened
STR	short tandem repeats
SUFU	Suppressor of Fused

development [11] and is deactivated in most body tissues after birth (with remaining regenerative functions in some) [12]. Signal transduction of canonical HH signaling occurs at the so-called primary cilium: After binding of one of the three known HH ligands (Sonic, Desert, Indian) to the transmembrane receptor Patched (PTCH), PTCH is inactivated. This inactivation results in the release of the second transmembrane receptor Smoothened (SMO). SMO governs the release of the glioma-associated oncogene (GLI) transcription factors by releasing GLI from their inhibiting factor Suppressor of Fused (SUFU). The released GLI transcription factors exhibit differential roles in HH signaling: While GLI1 and GLI2 mainly act as transcriptional activators, GLI3 acts as a transcriptional repressor [13,14].

Importantly, aberrant reactivation of HH signaling has been reported for a variety of tumor entities including RMS and MB, where it facilitates transcription of factors promoting cell cycle progression, proliferation and evasion of cell death such as apoptosis (i.e. by transcriptional activation of antiapoptotic BCL-2) [15,16]. Apoptosis is a form of programmed cell death [17] and evasion of apoptosis is a hallmark of human cancers that can be mediated by overexpression of antiapoptotic or by downregulation/inactivation of proapoptotic proteins [18]. Several studies found high expression levels of the antiapoptotic BCL-2 family proteins BCL-2, BCL-x_L and MCL-1 in RMS specimens [19–21]. Of note, switching the balance of pro- and antiapoptotic BCL-2 proteins towards proapoptotic BCL-2 proteins is regarded as a crucial step in overcoming tumor drug resistance [22]. Importantly, besides overexpressing antiapoptotic BCL-2 proteins, RMS have been reported to exhibit activated HH signaling on different levels of the pathway (i.e. canonically by ligand expression, non-canonically or by amplification of GLI1), in particular in a portion of ERMS and fusion-negative ARMS [23–25]. However, the prognostic impact of HH signaling activation in RMS remains unclear: While one study found that reactivation of the HH pathway is associated with poor survival in RMS [24], another study did not find any such association [26].

In an effort to target aberrant HH signaling in cancer, so-called HH pathway inhibitors (HPIs) have been developed that target different proteins in the signaling cascade [27]: Vismodegib and sonidegib target HH signaling on the level of SMO and have been approved for metastasized or otherwise untreatable basal cell carcinoma, which often harbors deactivating PTCH mutations, thereby resulting in an activation of HH signaling [28]. Furthermore, both compounds were evaluated in patients with advanced childhood MB. Here, tumor responses were only observed in tumors with HH signaling activation upstream of SMO [29,30]. Lastly, the Food & Drug Administration (FDA)-approved drug arsenic trioxide targets HH signaling at the level of GLI1 by directly binding this protein and inhibiting its transcriptional activity [31].

We recently reported that HH signaling suppresses the transcription of the proapoptotic BH3-only protein NOXA and that pharmacological or genetic abrogation of HH signaling reconstitutes NOXA expression in TP53-mutated RMS and MB cell lines [32]. However, we also found that NOXA induction in RMS cells treated with HPIs as a single agent is not sufficient to induce cell death on its own [33]. Since NOXA binds and thereby neutralizes the antiapoptotic protein MCL-1 [34] and RMS show high intrinsic MCL-1 levels [21], we hypothesized that transcriptional induction of NOXA by HPIs is insufficient to effectively neutralize MCL-1. Importantly, a novel BH3-mimetic named A-1210477 that specifically targets MCL-1 without increasing NOXA levels has been described recently [35]. In the present study, we tested the hypothesis that the combination treatment of A-1210477 and an HPI (that induces NOXA) may fully block MCL-1 function and thereby overcome intrinsic resistance of HH-driven cancers to HPIs.

2. Materials and methods

2.1. Cell culture and chemicals

The RMS cell line RH30 was obtained from Deutsche Sammlung von Mikroorganismen und Zellkulturen (DSMZ, Braunschweig, Germany), the RMS cell line RD was obtained from American Type Culture Collection (ATCC, Manassas, VA, USA) and the RMS cell line Kym-1 was obtained from Japanese Cancer Research Resources Bank (JCRB, Ibaraki, Osaka, Japan). The RMS cell line aRMS-CP was established from a patient with a PAX7-FOXO1-positive, pre-treated (carboplatin, epirubicin, vincristine, actinomycin-D, ifosfamide, etoposide) ARMS. The MB cell line DAOY was kindly provided by Marc Remke (Duesseldorf, Germany). Cell lines were authenticated by short tandem repeats (STR) profiles and negatively tested for mycoplasma contamination. RD, aRMS-CP and DAOY cells were maintained in DMEM GlutaMAX-I medium, RH30 and Kym-1 cells in RPMI 1640 GlutaMAX-I, both supplemented with 10% fetal calf serum (FCS), 1% penicillin/streptomycin and 1 mM sodium pyruvate (all Life Technologies, Inc., Darmstadt, Germany). RPMI 1640 medium was further supplemented with 25 mM HEPES for Kym-1 cells (Life Technologies, Inc., Darmstadt, Germany). GANT61 was purchased from Sigma-Aldrich (Taufkirchen, Germany), A-1210477 (MCL-1 inhibitor) was purchased from Active Biochem (Hongkong, China) and zVAD.fmk from Bachem (Heidelberg, Germany). If not indicated differently, all other chemicals were purchased from Sigma-Aldrich (Taufkirchen, Germany) or Carl Roth (Karlsruhe, Germany).

2.2. Determination of cell death and colony formation

Cell death was determined by fluorescence microscopy of propidium iodide (PI)-stained nuclei using ImageXpress Micro XLS system (Molecular Devices, Biberach an der Riss, Germany) or by flow cytometric analysis (FACSCanto II, BD Biosciences, Heidelberg, Germany) of DNA fragmentation of PI-stained nuclei as described previously [36].

For determination of colony formation, cells were seeded (200 cells/

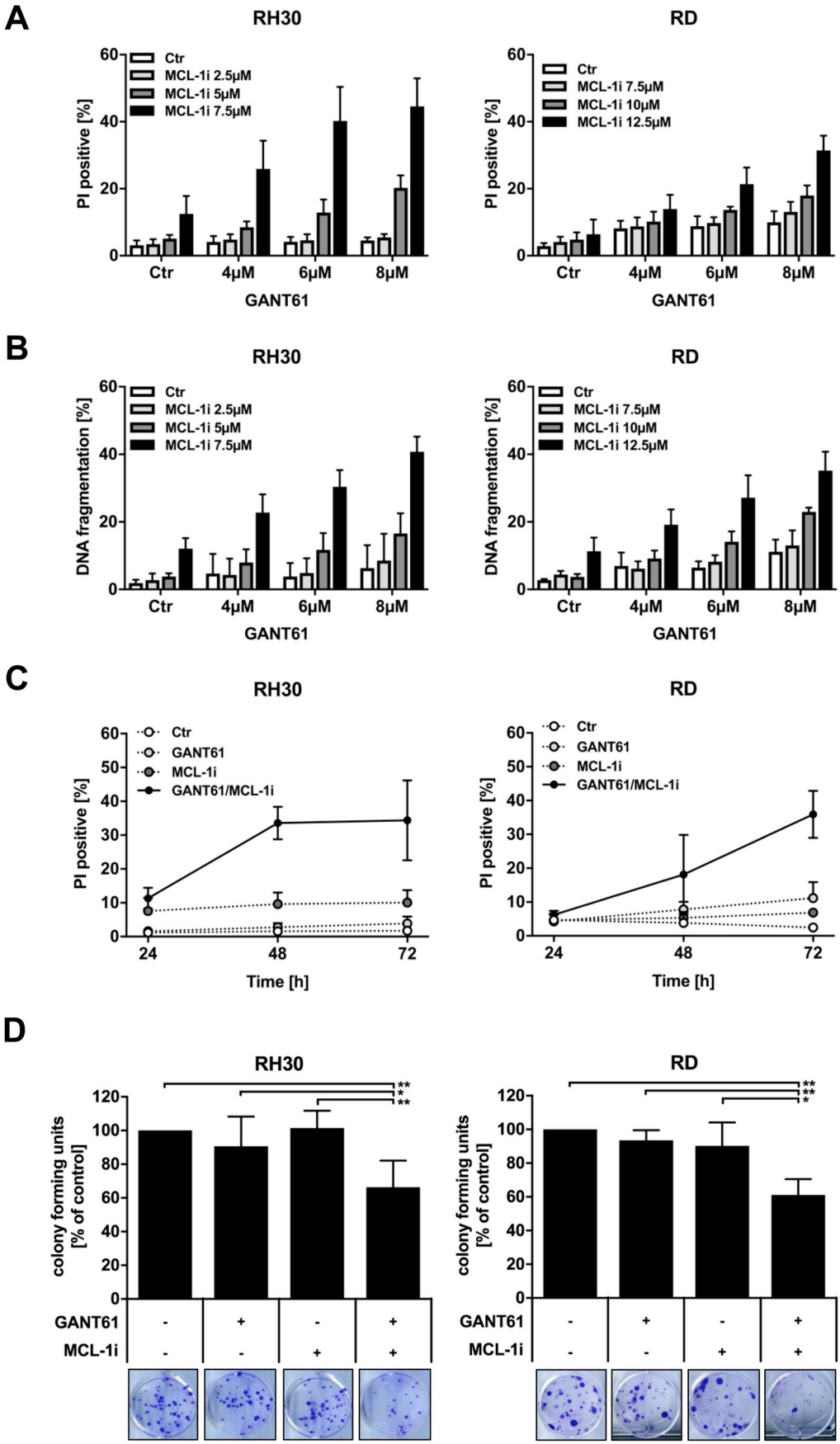

Fig. 1. Concomitant targeting of HH signaling and MCL-1 synergistically induces cell death in RMS cells. (A and B) RH30 and RD cells were treated with indicated concentrations of GANT61 and/or A-1210477 (MCL-1i) for 72 h. Cell death was determined by PI-stained nuclei using microscopy (A) or flow cytometry (B). Mean and SD of at least three independent experiments performed in triplicate are shown. (C) Cells were treated with 8 μM (RH30) or 6 μM (RD) GANT61 and/or 7.5 μM (RH30) or 12.5 μM (RD) A-1210477 (MCL-1i) for indicated time points. Cell death was determined by PI-stained nuclei using microscopy. Mean and SD of three independent experiments performed in triplicate are shown. (D) Cells were treated with 8 μM (RH30) or 6 μM (RD) GANT61 and/or 7.5 μM (RH30) or 12.5 μM (RD) A-1210477 (MCL-1i) for 10 h. Colony formation was assessed after 12–15 days. The number of colonies expressed as percentage of solvent-treated controls (top) and representative images (bottom) are shown. Mean and SD of at least three independent experiments performed in duplicate are shown. $*p < 0.05$, $**p < 0.01$.

well for RD cells, 100 cells/well for RH30 and DAOY cells) in six-well plates, allowed to settle overnight and treated with the according substances for 10 h. Thereafter, medium was changed, and colonies were stained after 12–15 days of growth with crystal violet solution (0.5% crystal violet, 30% ethanol, 3% formaldehyde). Colonies were counted and the percentage of colonies relative to solvent-treated controls was calculated.

2.3. Transient RNA interference

For transient knockdown of BIM, MCL-1 and NOXA by siRNA, cells were reversely transfected with 10 nM SilencerSelect siRNA (Invitrogen, Carlsbad, CA, USA) for control siRNA (4390843), BIM targeting siRNAs (s195011 (#1) and s195012 (#2)), MCL-1 targeting siRNAs (s8583 (#1) and s8584 (#2)) or NOXA targeting siRNAs (s10708 (#1), s10709 (#2) and s10710 (#3)), using Lipofectamine RNAi Max (Invitrogen, Carlsbad, CA, USA) and OptiMEM (Life Technologies, Inc., Darmstadt, Germany) according to the manufacturer's protocol. Knockdown efficiency was determined by Western blot analysis 24 h after reverse transfection (see 2.4.).

2.4. Western blot analysis

Western blot analysis was performed as described previously [37] using the following antibodies: α-TUBULIN (CP06, Calbiochem), BCL-x_L (2762S, Cell Signaling), BCL-2 (610539, BD Bioscience), mBCL-2 (anti-mouse) (33–6100, Invitrogen), β-ACTIN (A5441, Sigma-Aldrich), BIM (2819S, Cell Signaling), GAPDH (5G4-6C5, Hytest), GLI1 (2643S, Cell Signaling), MCL-1 (ADI-AAP-240F, Enzo Life Sciences), NOXA (ALX-804-408-C100, Enzo Life Sciences), VINCULIN (V9131, Sigma-Aldrich). Goat anti-mouse IgG conjugated to horseradish peroxidase (Santa Cruz Biotechnology, Santa Cruz, CA, USA) and enhanced chemiluminescence (Amersham Bioscience, Freiburg, Germany) or infrared dye-labeled secondary antibodies and infrared imaging (Odyssey Imaging System, LI-COR Bioscience, Bad Homburg, Germany) were used for detection. Representative blots of at least two independent experiments are shown.

2.5. Stable GLI1 knockdown

2.5.1. Generation of plasmids

The plasmids for stable lentiviral knockdown of GLI1 were generated by cloning the respective sequences into pLKO.1puro-TRC cloning vector (addgene #10878; [38]) according to the Addgene Protocol (Plasmid 10878. Protocol 1.0; http://www.addgene.org/tools/protocols/plko/#A). Briefly, suitable oligonucleotides were annealed and ligated into pLKO.1-TRC cloning cut with AgeI and EcoRI. Successful insertion was verified by Sanger sequencing of shRNA sequences. The shRNA sequences were retrieved from the RNAi consortium homepage (now Genetic Perturbation Platform; https://portals.broadinstitute.org/gpp/public/; [39]). The oligonucleotides sequences used for cloning are: CCGGCGTGAGCCTGAATCTGTGTATCTCGAGATACACAGATTCAGGCTCACGTTTTTG (GLI1_f); ATTCAAAAACGTGAGCCTGAATCTGTGTATCTCGAGATACACAGATTCAGGCTCACG (GLI1_r).

2.5.2. Production of lentiviral supernatant and transduction of RH30

Lentiviral supernatant was in principle generated according to the Addgene Protocol (Plasmid 10878. Protocol 1.0; http://www.addgene.org/tools/protocols/plko/#A). Briefly, HEK293T cells (70% confluent in six-well-plates) were transfected with the respective pLKO.1-shGLI plasmid or a scrambled pLKO.1-shCtrl (Sigma) together with the helper plasmids psPAX2 (Addgene plasmid 12260) and pMD.2G (Addgene plasmid 12259) using Fugene HD (Promega, Madison, WI, USA) according to the manufacturer's protocol. After 16 h of incubation, medium was changed to fresh medium and 24 h and 48 h later supernatant was collected, pooled and filtered through a 0.45 µm pore strainer to remove detached cells. The supernatant was used within one week of collection. For transduction, RH30 cells were grown to 70% confluency in a T25 flask. After removal of the culture medium, the viral supernatant was mixed 1:1 with fresh medium and added to the cells. To facilitate viral infection 8 µg/ml polybrene was added to the viral supernatant. After 24 h, the supernatant was removed and cells were supplied with fresh medium. After additional 24 h, cells were kept in medium containing 1 µg/ml puromycin for selection. Successful knockdown was validated using Western blot analysis (see 2.4.).

2.6. Overexpression of BCL-2 and MCL-1

For BCL-2 overexpression, Phoenix packaging cells were transfected with 20 µg of murine stem cell virus (pMSCV, Clontech, Mountain View, CA, USA) vector containing murine BCL-2 or empty vector (EV) using calcium phosphate transfection as described previously [40]. Stable cell lines were generated by lentiviral transduction and selected with 10 µg/ml Blasticidin (Invitrogen, Carlsbad, CA, USA). For stable expression of MCL-1, cells were transfected with 20 µg of pCMV-Tag3B plasmid containing MCL-1 or EV (kindly provided by Genentech (South San Francisco, CA, USA)) supplied with Lipofectamine 2000 (Life Technologies, Inc., Darmstadt, Germany) and selected with 0.5 mg/ml G418 as described previously [41]. Transfection efficiency was confirmed by Western blot analysis (see 2.4.).

2.7. Co-immunoprecipitation of BCL-2, BCL-x_L and MCL-1

Co-Immunoprecipitation of BCL-2, BCL-x_L and MCL-1 was performed in 400 µl lysates (using CHAPS lysis buffer (10 mM HEPES (pH 7.4); 150 mM NaCl; 1% CHAPS) supplemented with 1 mM protease inhibitor cocktail (Sigma-Aldrich, Taufkirchen, Germany) according to the manufacturer's protocol) containing 1 mg protein, which was incubated overnight at 4 °C with 1.25 µg hamster anti-BCL-2 antibody (551051, clone 6C8, BD Biosciences), 1 µg mouse anti-BCL-x_L antibody (MAB3121, clone 7B2.5, Millipore) or 2.5 µg rabbit anti-MCL-1 antibody (559027, clone 22, BD Biosciences). Antibodies were crosslinked to 30 µl pan-mouse IgG Dynabeads or Protein G Dynabeads (Life Technologies, Inc., Darmstadt, Germany) using 20 mM DMP prior to incubation. After incubation, samples were washed with CHAPS lysis buffer. Thereafter, the precipitate was analyzed for interaction with BCL-2, BCL-x_L, BIM and MCL-1 by Western blot analysis (see 2.4.).

2.8. Statistical analysis

Statistical significance was assessed by one-way or two-way ANOVA via GraphPad Prism software (version 7, GraphPad Software, CA, USA). Drug interactions were analyzed by the combination index (CI) method based on that described by Chou [42] using CalcuSyn software (Biosoft, Cambridge, UK). CI < 0.9 indicates synergism, 0.9–1.1 additivity and > 1.1 antagonism.

3. Results

3.1. Concomitant targeting of HH signaling and MCL-1 synergistically induces cell death in RMS cells

To test our hypothesis that concomitant inhibition of HH signaling and MCL-1 overcomes intrinsic resistance to HPIs and results in synergistic induction of cell death we treated two representative RMS cell lines (i.e. RH30 as a fusion gene positive ARMS and RD as a fusion gene negative ERMS) with the GLI1-targeting HPI GANT61 and the BH3-mimetic A-1210477 inhibiting MCL-1 (MCL-1i). Of note, combination treatment with GANT61 and A-1210477 cooperated to trigger cell death in both RH30 and RD cells, as determined by PI uptake (Fig. 1A). In contrast, single treatment with either GANT61 or A-1210477 resulted only in a minor increase in cell death (Fig. 1A). Calculation of CI

revealed a synergistic interaction of the two compounds (Suppl. Tab. 1A). We verified these findings by employing another cell death assay. Similarly, GANT61 and A-1210477 synergized to induce DNA fragmentation used as a typical marker of cell death (Fig. 1B and Suppl. Tab. 1B). A kinetic analysis revealed that the GANT61/A-1210477 combination triggered cell death in a time-dependent manner with the onset of cell death occurring after 24 h (Fig. 1C). To study the long-term efficacy of the combination treatment we performed colony formation assays. Importantly, GANT61/A-1210477 co-treatment resulted in a significant decrease in colony numbers in both RH30 and RD cells when compared to the untreated control or either single agent (Fig. 1D). We did not observe any significant changes in the distribution of cell cycle phases upon treatment in RH30 cells (Suppl. Fig. 2).

Since both RH30 and RD cell lines harbor an inactivating TP53 mutation [43], we extended our study to the TP53 wildtype RMS cell line Kym-1 [44] to test if the TP53 status influences the susceptibility to

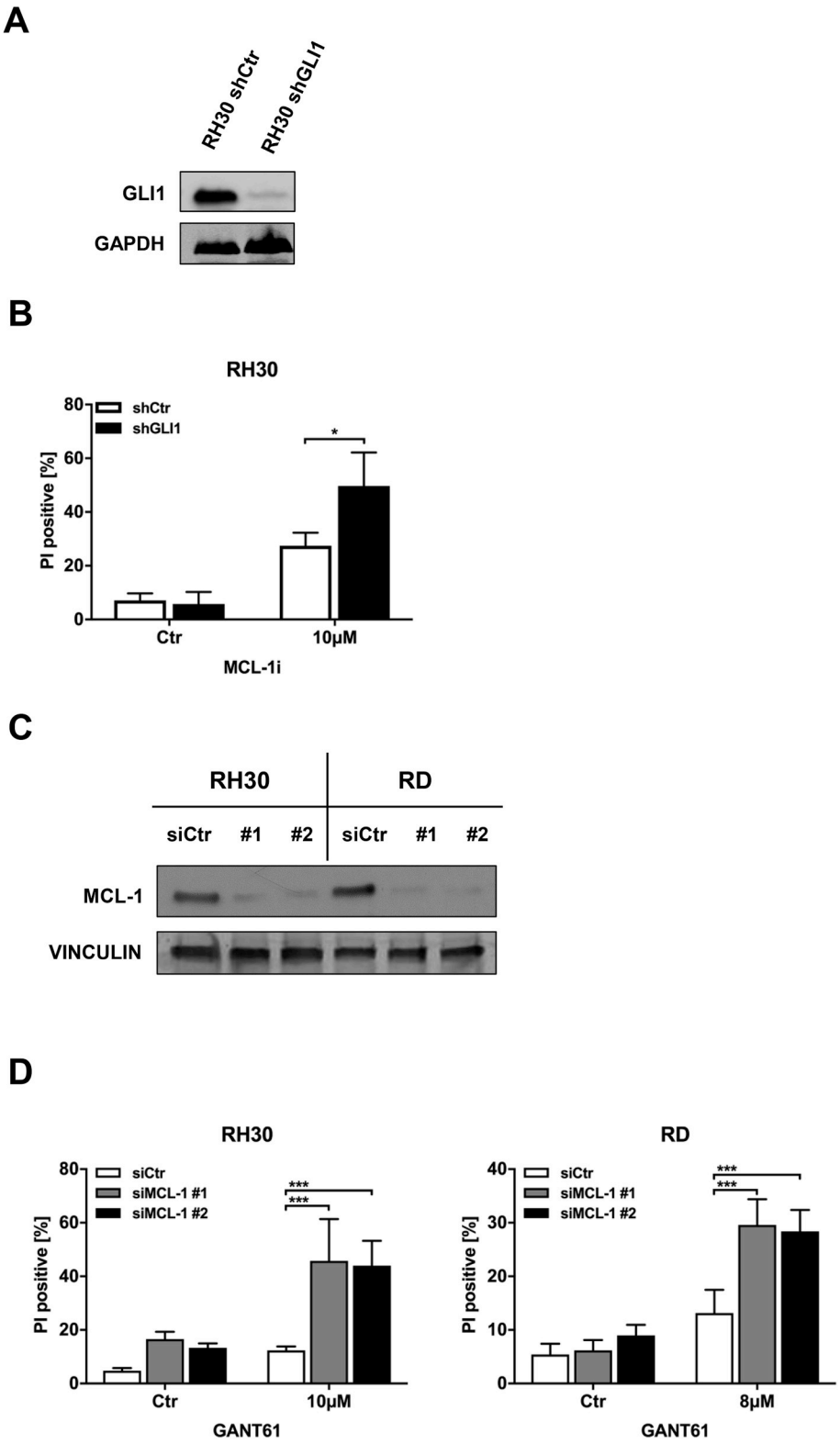

Fig. 2. Pharmacological and genetic blockade of GLI1 and MCL-1 act in concert to induce cell death. (A and B) RH30 cells were lentivirally transduced to knock down GLI1. GLI1 expression was assessed by Western blot analysis, GAPDH served as loading control (A). Transduced RH30 cells were treated with 10 μM A-1210477 (MCL-1i) for 72 h. Cell death was determined by PI-stained nuclei using microscopy. Mean and SD of three independent experiments performed in triplicate are shown (B). $^{*}p < 0.05$. (C and D) RH30 and RD cells were transiently transfected with siRNA against MCL-1 or non-targeting control siRNA. Expression of MCL-1 was assessed by Western blot analysis, VINCULIN served as loading control (C). 24 h after reverse transfection, cells were treated with 10 μM (RH30) or 8 μM (RD) GANT61 for 48 h. Cell death was determined by PI-stained nuclei using microscopy. Mean and SD of three independent experiments performed in triplicate are shown (D). $^{***}p < 0.001$.

the GANT61/A-1210477 combination. However, GANT61 and A-1210477 similarly cooperated to engage cell death in TP53 wildtype Kym-1 cells (Suppl. Fig. 1A). To explore the translational relevance of our findings we extended our study to a primary RMS cell culture (i.e. aRMS-CP cells). Of note, GANT61/A-1210477 co-treatment was significantly more effective to induce cell death compared to either treatment alone (Suppl. Fig. 1B).

To test if this synergism of GLI1 and MCL-1 inhibitors is tumor entity-specific we extended our experiments to the TP53-mutated MB cell line DAOY [45]. MB are known to exhibit hyperactivation of HH signaling in a subgroup of cases (the so-called sonic HH (SHH) subgroup) [46]. Of note, GANT61 and A-1210477 acted in concert to synergistically cause cell death in DAOY cells as well (Suppl. Fig. 1C and 1D). In addition, GANT61/A-1210477 co-treatment significantly suppressed colony formation in DAOY cells (Suppl. Fig. 1E).

Taken together, this set of experiments shows that GANT61 and A-1210477 synergistically induce cell death in RMS cells regardless of their TP53 status.

3.2. Pharmacological and genetic blockade of GLI1 and MCL-1 act in concert to induce cell death

To further test our hypothesis that parallel inhibition of HH signaling and MCL-1 causes synergistic induction of cell death we combined genetic and pharmacological abrogation of either GLI1 or MCL-1 protein. To this end, we silenced GLI1 by shRNA-mediated knockdown in RH30 cells which harbor a GLI1 amplification [26] (Fig. 2A). Importantly, GLI1 silencing significantly increased cell death when combined with pharmacological inhibition of MCL-1, compared to control cells expressing a non-targeting shRNA (Fig. 2B). *Vice versa*, siRNA-mediated genetic silencing of MCL-1 in RH30 and RD cells (Fig. 2C) in combination with pharmacological inhibition of GLI1 resulted in significantly increased cell death compared to control cells (Fig. 2D).

Taken together, these findings show that pharmacological and genetic inhibition of GLI1 and MCL-1 act in concert to induce cell death. These findings provide evidence showing that GANT61/A-1210477-induced cell death indeed results from specific inhibition of GLI1 and MCL-1 rather than from off-target effects of these compounds.

3.3. MCL-1i triggers BIM translocating from MCL-1 to BCL-x_L and BCL-2

Since RMS have been reported to express high levels of MCL-1 [21], we hypothesized that GANT61/A-1210477-induced cell death is mediated by a combined blockade of MCL-1 by pharmacological inhibition (by A-1210477) and NOXA induction (by GANT61, as previously reported by our group [32,33]) which binds to and thereby neutralizes MCL-1 [34], resulting in increased release of BIM from MCL-1. To test this hypothesis we performed co-immunoprecipitation experiments of the antiapoptotic proteins MCL-1, BCL-2 and BCL-x_L and analyzed their binding to BIM. Interestingly, A-1210477 decreased the binding of BIM to MCL-1 accompanied by increased binding of BIM to BCL-x_L and also to BCL-2, in particular upon co-treatment of GANT61 and A-1210477, in both cell lines (Fig. 3A and B). This indicates that A-1210477 releases BIM from MCL-1 which then shuttles to BCL-x_L and also to BCL-2. We also observed that treatment with A-1210477 caused an accumulation of MCL-1 which is in line with a previous report [35].

3.4. BIM and NOXA contribute to GANT61/A-1210477-induced cell death

To test if the BH3-only proteins BIM and NOXA are crucial for cell death induced by the combination of GANT61 and A-1210477 we silenced BIM (Fig. 4A) and NOXA (Fig. 4C) by siRNA. Of note, silencing of BIM (Fig. 4B) as well as silencing of NOXA (Fig. 4D) significantly decreased GANT61/A-1210477-induced cell death in both RH30 and RD cells. These findings show that BIM and NOXA both contribute to GANT61/A-1210477-induced cell death and suggest that the translocation of BIM from MCL-1 to BCL-x_L and BCL-2 is indeed crucial for mediating cell death.

3.5. Overexpression of BCL-2 or MCL-1 rescues cells from GANT61/A-1210477-induced cell death

Since our co-immunoprecipitation experiments suggested that blockade of antiapoptotic proteins occurs upon combination treatment of GANT61/A-1210477, we asked whether this blockade is indeed crucial for cell death induction. We therefore overexpressed BCL-2 and MCL-1 in RH30 and RD cells. Importantly, BCL-2 overexpression significantly rescued both RH30 and RD cells from GANT61/A-1210477-triggered cell death (Fig. 5A and B). Also, we observed a significant rescue from cell death in RH30 cells treated with A-1210477 alone and in RD cells treated with GANT61 alone upon ectopic BCL-2 expression (data not shown). Similarly, ectopic expression of MCL-1 provided significant protection against cell death upon GANT61/A-1210477 co-treatment in both cell lines (Fig. 5C and D). Also, we observed a significant rescue from cell death in RD cells treated with GANT61 alone upon ectopic MCL-1 expression (data not shown). This suggests that the blockade of antiapoptotic BCL-2 and MCL-1 is crucial for cell death induction by GANT61/A-1210477.

3.6. Caspase activity contributes to GANT61/A-1210477-induced cell death

To test if cells undergo caspase-dependent apoptosis upon co-

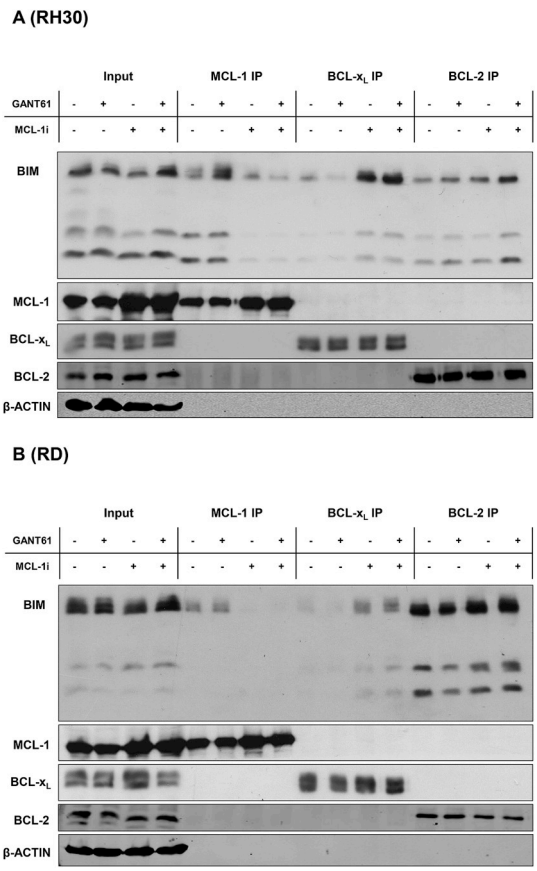

Fig. 3. MCL-1i triggers BIM translocating from MCL-1 to BCL-x_L and BCL-2. (A and B) RH30 (A) and RD (B) cells were treated with 8 μM (RH30) or 6 μM (RD) GANT61 and/or 7.5 μM (RH30) or 12.5 μM (RD) A-1210477 (MCL-1i) for 20 h and MCL-1, BCL-x_L and BCL-2 immunoprecipitated. The precipitate was analyzed for BIM, MCL-1, BCL-x_L and BCL-2 expression by Western blot analysis. β-ACTIN served as loading control.

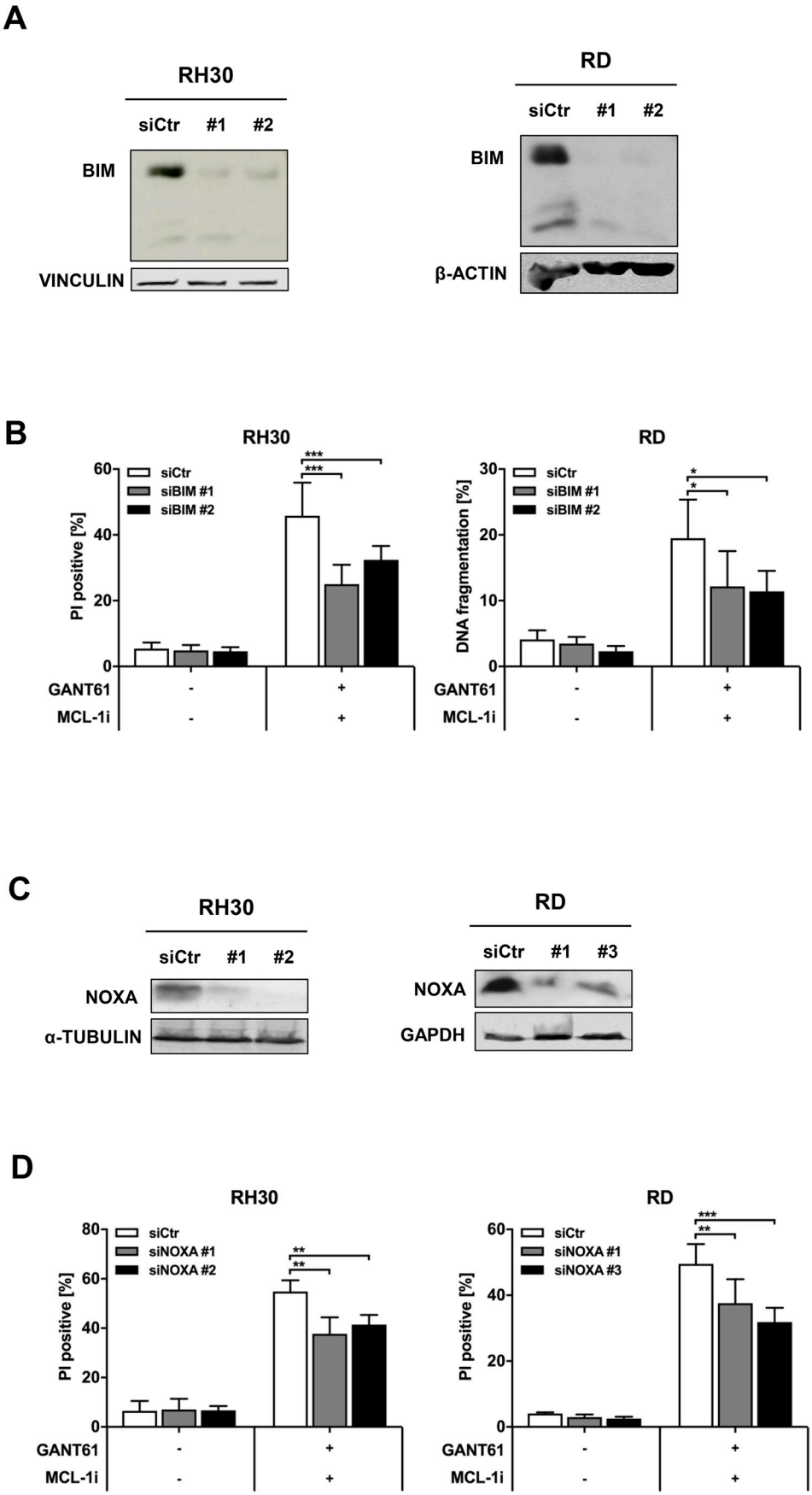

Fig. 4. BIM and NOXA contribute to GANT61/A-1210477-induced cell death. (A) RH30 and RD cells were transiently transfected with siRNA against BIM or non-targeting control siRNA. Expression of BIM was assessed by Western blot analysis, α-VINCULIN or β-ACTIN served as loading control. (B) Cells were treated with 6 μM (RH30 and RD) GANT61 and 6 μM (RH30) or 12.5 μM (RD) A-1210477 (MCL-1i) for 48 h (RD) or 72 h (RH30). Cell death was determined by PI-stained nuclei using microscopy (RH30) or flow cytometry (RD). Mean and SD of at least three independent experiments performed in triplicate are shown. $*p < 0.05$, $***p < 0.001$. (C) RH30 and RD cells were transiently transfected with siRNA against NOXA or non-targeting control siRNA. Expression of NOXA was assessed by Western blot analysis, α-TUBULIN or GAPDH served as loading control. (D) Cells were treated with 6 μM (RH30 and RD) GANT61 and 6 μM (RH30) or 12.5 μM (RD) A-1210477 (MCL-1i) for 72 h. Cell death was determined by PI-stained nuclei using microscopy (RH30) or flow cytometry (RD). Mean and SD of three independent experiments performed in triplicate are shown. $*p < 0.05$; $**p < 0.01$, $***p < 0.001$.

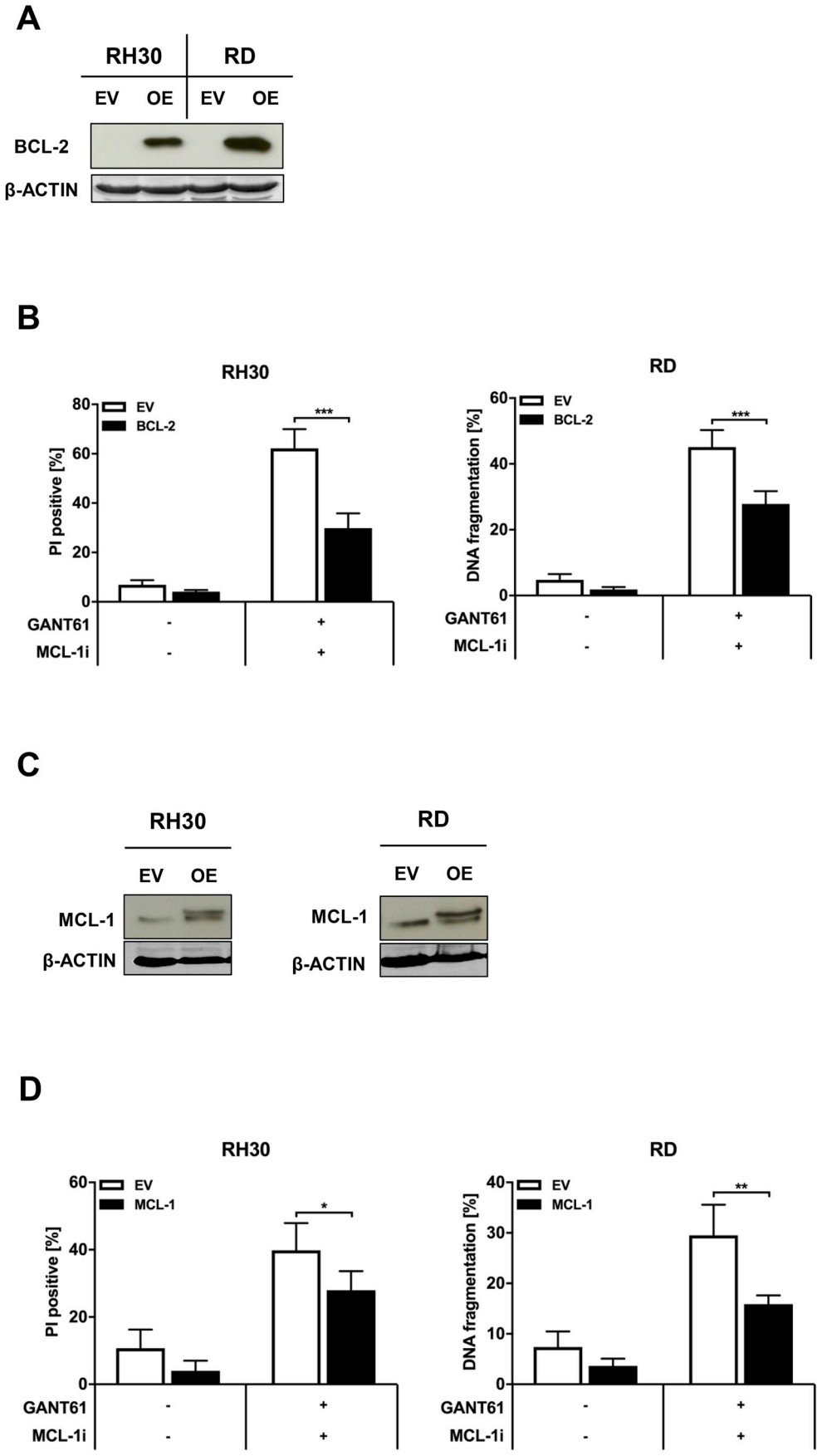

Fig. 5. Overexpression of BCL-2 or MCL-1 rescues cells from GANT61/A-1210477-induced cell death. (A–B) RH30 and RD cells were lentivirally transduced to overexpress murine BCL-2 or EV and expression of BCL-2 was assessed by Western blot analysis, β-ACTIN served as loading control (A). Transduced cells were treated with 8 μM (RH30) or 6 μM (RD) GANT61 and 7.5 μM (RH30) or 12.5 μM (RD) A-1210477 (MCL-1i) for 72 h. Cell death was determined by PI-stained nuclei using microscopy (RH30) or flow cytometry (RD). Mean and SD of three independent experiments performed in triplicate are shown. $***p < 0.001$. (C–D) RH30 and RD cells were transfected to overexpress MCL-1 or EV and expression of MCL-1 was assessed by Western blot analysis, β-ACTIN served as loading control (C). Transfected cells were treated with 8 μM (RH30) or 6 μM (RD) GANT61 and 7.5 μM (RH30) or 12.5 μM (RD) A-1210477 (MCL-1i) for 72 h. Cell death was determined by PI-stained nuclei using microscopy. Mean and SD of at least three independent experiments performed in triplicate are shown.

treatment of GANT61 and A-1210477 as a consequence of an altered balance of pro- and antiapoptotic BCL-2 protein family members we blocked caspase function by adding the pan-caspase inhibitor zVAD.fmk. Of note, zVAD.fmk significantly reduced GANT61/A-1210477-stimulated cell death in RH30 and also in RD cells (although to a lesser extent) (Fig. 6A and B). Furthermore, we observed a minor albeit significant rescue from cell death induced by A-1210477 alone in RH30 cells upon zVAD.fmk addition (data not shown). This finding indicates that caspase activity contributes to GANT61/A-1210477-induced cell death.

4. Discussion

In the present study, we show that concomitant pharmacological targeting of HH signaling and MCL-1 synergistically induces cell death in RMS cells, whereas either compound alone exerts minimal or moderate effects. This conclusion is further supported by combined genetic and pharmacological inhibition, demonstrating that co-treatment of GANT61 and A-1210477 indeed relies on inhibition of GLI1 (by GANT61) and MCL-1 (by A-1210477).

Mechanistically, we show that A-1210477 triggers the release of BIM from MCL-1 and its re-shuttling to BCL-x_L and BCL-2, while GANT61 results in NOXA induction as previously reported by our group [32,33]. Thereby, A-1210477 and GANT61 act in concert to shift the balance of pro- and antiapoptotic BCL-2 family proteins in favor of apoptosis, facilitating the induction of cell death. In support of this model, genetic silencing of proapoptotic BIM or NOXA rescued cells from GANT61/A-1210477-induced cell death. *Vice versa*, overexpression of antiapoptotic BCL-2 or MCL-1 protected cells from GANT61/A-1210477-triggered cell death. These findings highlight that the shift in the balance of pro- and antiapoptotic BCL-2 family proteins is critical to ultimately engage cell death.

Of note, BIM has been implicated in the execution of cell death for a subset of RMS tumors [47], further highlighting the rationale to employ drugs in RMS therapy that may result in an increase of unbound BIM (such as MCL-1 inhibitors). Notably, abrogation of caspase function by addition of the pan-caspase inhibitor zVAD.fmk resulted in a significant rescue from cell death conferred by combination treatment, indicating that cells ultimately undergo cell death that largely depends on caspases. However, as zVAD.fmk was unable to completely block cell death, caspase-independent forms of cell death may also contribute to cell death upon the combination treatment of GANT61 and A-1210477.

In line with previous studies, we observed an increase of MCL-1 protein levels upon treatment with A-1210477 [35]. Besides neutralizing MCL-1, A-1210477 may potentially also stabilize MCL-1 due to conformational changes in its protein structure, rendering it less prone to degradation.

Taken together, the results of the present study show that single-agent blockade of HH signaling is not sufficient to induce cell death in RMS, which goes in line with our previous studies [33,48]. Intriguingly, the combination treatment including the GLI1 targeting agent GANT61 proved to be more efficacious in RH30 than in RD cells, although RH30 cells harbor a GLI1 amplification, resulting in higher GLI1 protein levels than in RD cells [23]. We hypothesize that RH30 cells may be more dependent on the transcriptional activity of GLI1 and are therefore more sensitive to the combination therapy. Hence, we limited our efforts in combining genetic abrogation of HH signaling (by shRNA-mediated knockdown) and pharmacological abrogation of MCL-1 (by A-1210477) to this cell line. However, future studies could employ cell lines derived from other tumor entities that show elevated GLI1 expression as a result of an amplification to further investigate this putative dependency. Furthermore, it may be of interest to determine if the combination treatment with GANT-61/A-1210477 shows increased potential to induce myogenic differentiation in RMS cells compared to single-agent HH pathway inhibitors [49,50].

Moreover, the combination treatment showed efficacy in RMS cells regardless of embryonal or alveolar histology or TP53 status (RH30 and RD with defective TP53 [43], Kym-1 with functional TP53 [44]). Of note, NOXA is a *bona fide* target gene of TP53 [51] and cell death induction by GANT61 and A-1210477 partially depended on NOXA. Of

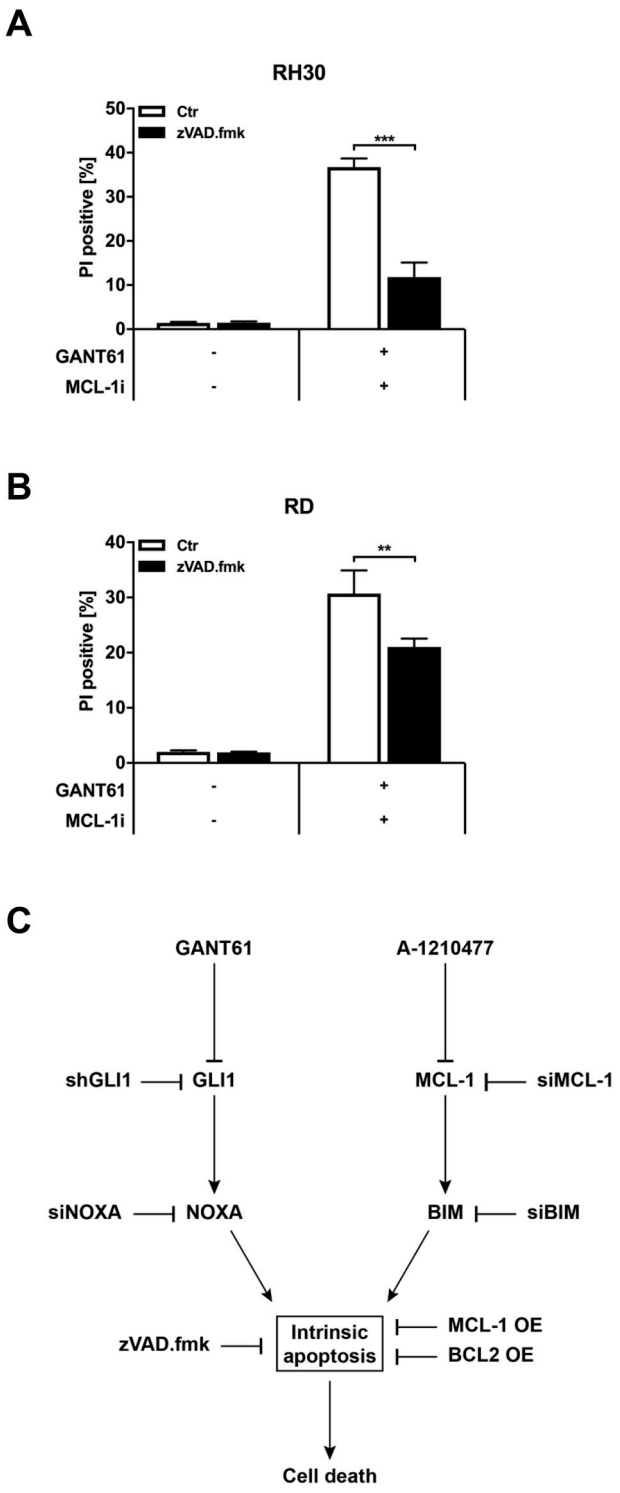

Fig. 6. Caspase activity contributes to GANT61/A-1210477-induced cell death. (A–B) Cells were treated with 8 μM (RH30) (A) or 6 μM (RD) (B) GANT61 and 7.5 μM (RH30) or 12.5 μM (RD) A-1210477 (MCL-1i) for 48 h (RH30) or 72 h (RD). Cell death was determined by PI-stained nuclei using microscopy. Mean and SD of three independent experiments performed in triplicate are shown. $^{**}p < 0.01$, $^{***}p < 0.001$. (C) Schematic representation of the results.

note, TAp73 might substitute for the lost TP53 function to induce NOXA upon GANT61/A-1210477 co-treatment, in line with our recent report [32]. These findings support the notion that the combination treatment of GANT61/A-1210477 may be employed for the treatment of patients with RMS, since ARMS usually do not display TP53 mutations (contrary to the ARMS cell line RH30), while ERMS commonly harbor mutations in this gene or other inactivating alterations in its regulation (i.e. amplification of TP53 inactivator MDM2) [9].

Besides RMS, a combination therapy using HPI and MCL-1 inhibitors could also prove to be a promising therapeutic avenue for high-risk MB patients, as the combination of GANT61 and A-1210477 also potently triggered cell death in TP53-mutated MB cells. A subgroup of MB exhibits HH activation (the so-called SHH subgroup [46]) and patients in the SHH group MB who also carry a TP53 germline mutation (resulting in Li-Fraumeni syndrome) face a particularly poor prognosis [52]. Considering further clinical translation, it has to be stated that in the present study relatively high concentrations of A-1210477 (up to 20 μM) were necessary to induce cell death upon combination treatment. Interestingly, Leverson et al. described inhibitory concentrations for A-1210477 in the micromolar range in other cell lines with high MCL-1 levels, potentially indicating a limited efficacy of this compound [35]. Importantly, novel MCL-1 inhibitors have recently been described (e.g. AZD5991 [53] and S63845 [54]) which showed a higher efficacy in blocking MCL-1 function. Furthermore, the study by Kotschy et al. also illustrated the limited toxicity of S63845 in mice, highlighting the potential this compound might have in treating patients with cancer [54].

In conclusion, our study identifies a synergistic antitumor activity of GLI1- and MCL-1-targeting agents. These findings may have important implications for the development of novel therapeutic strategies for patients suffering from HH-driven cancers.

Conflicts of interest

None to declare.

Acknowledgments

We thank C. Hugenberg for expert secretarial assistance. This work was supported by grants from the Else Kröner-Fresenius-Stiftung (to M.T.M. and S.F.), German Cancer Aid (to S.F., T.K.) and BMBF (to S.F., T.K.).

Appendix A. Supplementary data

Supplementary data to this article can be found online at https://doi.org/10.1016/j.canlet.2019.08.012.

References

[1] S. Kramer, A.T. Meadows, P. Jarrett, A.E. Evans, Incidence of childhood cancer: experience of a decade in a population-based registry, J. Natl. Cancer Inst. 70 (1983) 49–55.
[2] W.A. Newton Jr., E.H. Soule, A.B. Hamoudi, H.M. Reiman, H. Shimada, M. Beltangady, et al., Histopathology of childhood sarcomas, Intergroup Rhabdomyosarcoma Studies I and II: clinicopathologic correlation, J. Clin. Oncol. 6 (1988) 67–75.
[3] O. Oberlin, A. Rey, E. Lyden, G. Bisogno, M.C. Stevens, W.H. Meyer, et al., Prognostic factors in metastatic rhabdomyosarcomas: results of a pooled analysis from United States and European cooperative groups, J. Clin. Oncol. 26 (2008) 2384–2389.
[4] J. Abraham, Y. Nunez-Alvarez, S. Hettmer, E. Carrio, H.I. Chen, K. Nishijo, et al., Lineage of origin in rhabdomyosarcoma informs pharmacological response, Genes Dev. 28 (2014) 1578–1591.
[5] D. Driman, P.S. Thorner, M.L. Greenberg, S. Chilton-MacNeill, J. Squire, MYCN gene amplification in rhabdomyosarcoma, Cancer 73 (1994) 2231–2237.
[6] L. Toffolatti, E. Frascella, V. Ninfo, C. Gambini, M. Forni, M. Carli, et al., MYCN expression in human rhabdomyosarcoma cell lines and tumour samples, J. Pathol. 196 (2002) 450–458.
[7] F.G. Barr, F. Duan, L.M. Smith, D. Gustafson, M. Pitts, S. Hammond, et al., Genomic and clinical analyses of 2p24 and 12q13-q14 amplification in alveolar rhabdomyosarcoma: a report from the Children's Oncology Group, Genes Chromosomes Cancer 48 (2009) 661–672.
[8] G. Merlino, L.J. Helman, Rhabdomyosarcoma–working out the pathways, Oncogene 18 (1999) 5340–5348.
[9] J.F. Shern, L. Chen, J. Chmielecki, J.S. Wei, R. Patidar, M. Rosenberg, et al., Comprehensive genomic analysis of rhabdomyosarcoma reveals a landscape of alterations affecting a common genetic axis in fusion-positive and fusion-negative tumors, Cancer Discov. 4 (2014) 216–231.
[10] S. Malempati, D.S. Hawkins, Rhabdomyosarcoma: review of the children's Oncology group (COG) soft-tissue sarcoma committee experience and rationale for current COG studies, Pediatr. Blood Cancer 59 (2012) 5–10.
[11] M. Varjosalo, J. Taipale, Hedgehog: functions and mechanisms, Genes Dev. 22 (2008) 2454–2472.
[12] P.A. Beachy, S.S. Karhadkar, D.M. Berman, Tissue repair and stem cell renewal in carcinogenesis, Nature 432 (2004) 324–331.
[13] T. Eichberger, V. Sander, H. Schnidar, G. Regl, M. Kasper, C. Schmid, et al., Overlapping and distinct transcriptional regulator properties of the GLI1 and GLI2 oncogenes, Genomics 87 (2006) 616–632.
[14] K.E. Ryan, C. Chiang, Hedgehog secretion and signal transduction in vertebrates, J. Biol. Chem. 287 (2012) 17905–17913.
[15] S.J. Scales, F.J. de Sauvage, Mechanisms of Hedgehog pathway activation in cancer and implications for therapy, Trends Pharmacol. Sci. 30 (2009) 303–312.
[16] B. Stecca, I.A.A. Ruiz, Context-dependent regulation of the GLI code in cancer by HEDGEHOG and non-HEDGEHOG signals, J. Mol. Cell Biol. 2 (2010) 84–95.
[17] S. Fulda, K.M. Debatin, Extrinsic versus intrinsic apoptosis pathways in anticancer chemotherapy, Oncogene 25 (2006) 4798–4811.
[18] S. Fulda, Tumor resistance to apoptosis, Int. J. Cancer 124 (2009) 511–515.
[19] P.M. Armistead, J. Salganick, J.S. Roh, D.M. Steinert, S. Patel, M. Munsell, et al., Expression of receptor tyrosine kinases and apoptotic molecules in rhabdomyosarcoma: correlation with overall survival in 105 patients, Cancer 110 (2007) 2293–2303.
[20] C.M. Margue, M. Bernasconi, F.G. Barr, B.W. Schafer, Transcriptional modulation of the anti-apoptotic protein BCL-XL by the paired box transcription factors PAX3 and PAX3/FKHR, Oncogene 19 (2000) 2921–2929.
[21] L. Pazzaglia, A. Chiechi, A. Conti, G. Gamberi, G. Magagnoli, C. Novello, et al., Genetic and molecular alterations in rhabdomyosarcoma: mRNA overexpression of MCL1 and MAP2K4 genes, Histol. Histopathol. 24 (2009) 61–67.
[22] L.D. Walensky, BCL-2 in the crosshairs: tipping the balance of life and death, Cell Death Differ. 13 (2006) 1339–1350.
[23] W.M. Roberts, E.C. Douglass, S.C. Peiper, P.J. Houghton, A.T. Look, Amplification of the gli gene in childhood sarcomas, Cancer Res. 49 (1989) 5407–5413.
[24] A. Zibat, E. Missiaglia, A. Rosenberger, K. Pritchard-Jones, J. Shipley, H. Hahn, et al., Activation of the hedgehog pathway confers a poor prognosis in embryonal and fusion gene-negative alveolar rhabdomyosarcoma, Oncogene 29 (2010) 6323–6330.
[25] A. Almazan-Moga, P. Zarzosa, C. Molist, P. Velasco, J. Pyczek, K. Simon-Keller, et al., Ligand-dependent Hedgehog pathway activation in Rhabdomyosarcoma: the oncogenic role of the ligands, Br. J. Canc. 117 (2017) 1314–1325.
[26] J.G. Pressey, J.R. Anderson, D.K. Crossman, J.C. Lynch, F.G. Barr, Hedgehog pathway activity in pediatric embryonal rhabdomyosarcoma and undifferentiated sarcoma: a report from the Children's Oncology Group, Pediatr. Blood Cancer 57 (2011) 930–938.
[27] J.A. Low, F.J. de Sauvage, Clinical experience with Hedgehog pathway inhibitors, J. Clin. Oncol. 28 (2010) 5321–5326.
[28] R. Danhof, K. Lewis, M. Brown, Small molecule inhibitors of the hedgehog pathway in the treatment of basal cell carcinoma of the skin, Am. J. Clin. Dermatol. 19 (2018) 195–207.
[29] M.W. Kieran, J. Chisholm, M. Casanova, A.A. Brandes, I. Aerts, E. Bouffet, et al., Phase I study of oral sonidegib (LDE225) in pediatric brain and solid tumors and a phase II study in children and adults with relapsed medulloblastoma, Neuro Oncol. 19 (2017) 1542–1552.
[30] G.W. Robinson, B.A. Orr, G. Wu, S. Gururangan, T. Lin, I. Qaddoumi, et al., Vismodegib exerts targeted efficacy against recurrent sonic hedgehog-subgroup medulloblastoma: results from phase II pediatric brain tumor consortium studies PBTC-025B and PBTC-032, J. Clin. Oncol. 33 (2015) 2646–2654.
[31] E.M. Beauchamp, L. Ringer, G. Bulut, K.P. Sajwan, M.D. Hall, Y.C. Lee, et al., Arsenic trioxide inhibits human cancer cell growth and tumor development in mice by blocking Hedgehog/GLI pathway, J. Clin. Investig. 121 (2011) 148–160.
[32] M.T. Meister, C. Boedicker, T. Klingebiel, S. Fulda, Hedgehog signaling negatively co-regulates BH3-only protein Noxa and TAp73 in TP53-mutated cells, Cancer Lett. 429 (2018) 19–28.
[33] U. Graab, H. Hahn, S. Fulda, Identification of a novel synthetic lethality of combined inhibition of hedgehog and PI3K signaling in rhabdomyosarcoma, Oncotarget 6 (2015) 8722–8735.
[34] C. Ploner, R. Kofler, A. Villunger, Noxa: at the tip of the balance between life and death, Oncogene 27 (Suppl 1) (2008) S84–S92.
[35] J.D. Leverson, H. Zhang, J. Chen, S.K. Tahir, D.C. Phillips, J. Xue, et al., Potent and selective small-molecule MCL-1 inhibitors demonstrate on-target cancer cell killing activity as single agents and in combination with ABT-263 (navitoclax), Cell Death Dis. 6 (2015) e1590.
[36] E. Preuss, M. Hugle, R. Reimann, M. Schlecht, S. Fulda, Pan-mammalian target of rapamycin (mTOR) inhibitor AZD8055 primes rhabdomyosarcoma cells for ABT-737-induced apoptosis by down-regulating Mcl-1 protein, J. Biol. Chem. 288 (2013) 35287–35296.
[37] S. Fulda, H. Sieverts, C. Friesen, I. Herr, K.M. Debatin, The CD95 (APO-1/Fas)

system mediates drug-induced apoptosis in neuroblastoma cells, Cancer Res. 57 (1997) 3823–3829.
[38] J. Moffat, D.A. Grueneberg, X. Yang, S.Y. Kim, A.M. Kloepfer, G. Hinkle, et al., A lentiviral RNAi library for human and mouse genes applied to an arrayed viral high-content screen, Cell 124 (2006) 1283–1298.
[39] X. Yang, J.S. Boehm, X. Yang, K. Salehi-Ashtiani, T. Hao, Y. Shen, et al., A public genome-scale lentiviral expression library of human ORFs, Nat. Methods 8 (2011) 659–661.
[40] U. Heinicke, S. Fulda, Chemosensitization of rhabdomyosarcoma cells by the histone deacetylase inhibitor SAHA, Cancer Lett. 351 (2014) 50–58.
[41] M. Hugle, K. Belz, S. Fulda, Identification of synthetic lethality of PLK1 inhibition and microtubule-destabilizing drugs, Cell Death Differ. 22 (2015) 1946–1956.
[42] T.C. Chou, Drug combination studies and their synergy quantification using the Chou-Talalay method, Cancer Res. 70 (2010) 440–446.
[43] C.A. Felix, C.C. Kappel, T. Mitsudomi, M.M. Nau, M. Tsokos, G.D. Crouch, et al., Frequency and diversity of p53 mutations in childhood rhabdomyosarcoma, Cancer Res. 52 (1992) 2243–2247.
[44] J. Muret, M. Hasmim, I. Stasik, A. Jalil, A. Mallavialle, A. Nanbakhsh, et al., Attenuation of soft-tissue sarcomas resistance to the cytotoxic action of TNF-alpha by restoring p53 function, PLoS One 7 (2012) e38808.
[45] R.L. Saylors 3rd, D. Sidransky, H.S. Friedman, S.H. Bigner, D.D. Bigner, B. Vogelstein, et al., Infrequent p53 gene mutations in medulloblastomas, Cancer Res. 51 (1991) 4721–4723.
[46] M.D. Taylor, P.A. Northcott, A. Korshunov, M. Remke, Y.J. Cho, S.C. Clifford, et al., Molecular subgroups of medulloblastoma: the current consensus, Acta Neuropathol. 123 (2012) 465–472.
[47] M. Wachtel, J. Rakic, M. Okoniewski, P. Bode, F. Niggli, B.W. Schafer, FGFR4 signaling couples to Bim and not Bmf to discriminate subsets of alveolar rhabdomyosarcoma cells, Int. J. Cancer 135 (2014) 1543–1552.
[48] M.T. Meister, C. Boedicker, U. Graab, M. Hugle, H. Hahn, T. Klingebiel, et al., Arsenic trioxide induces Noxa-dependent apoptosis in rhabdomyosarcoma cells and synergizes with antimicrotubule drugs, Cancer Lett. 381 (2016) 287–295.
[49] S. Satheesha, G. Manzella, A. Bovay, E.A. Casanova, P.K. Bode, R. Belle, et al., Targeting hedgehog signaling reduces self-renewal in embryonal rhabdomyosarcoma, Oncogene 35 (2016) 2020–2030.
[50] M. Koleva, R. Kappler, M. Vogler, A. Herwig, S. Fulda, H. Hahn, Pleiotropic effects of sonic hedgehog on muscle satellite cells, Cell. Mol. Life Sci. 62 (2005) 1863–1870.
[51] E. Oda, R. Ohki, H. Murasawa, J. Nemoto, T. Shibue, T. Yamashita, et al., Noxa, a BH3-only member of the Bcl-2 family and candidate mediator of p53-induced apoptosis, Science 288 (2000) 1053–1058.
[52] N. Zhukova, V. Ramaswamy, M. Remke, E. Pfaff, D.J. Shih, D.C. Martin, et al., Subgroup-specific prognostic implications of TP53 mutation in medulloblastoma, J. Clin. Oncol. 31 (2013) 2927–2935.
[53] A.E. Tron, M.A. Belmonte, A. Adam, B.M. Aquila, L.H. Boise, E. Chiarparin, et al., Discovery of Mcl-1-specific inhibitor AZD5991 and preclinical activity in multiple myeloma and acute myeloid leukemia, Nat. Commun. 9 (2018) 5341.
[54] A. Kotschy, Z. Szlavik, J. Murray, J. Davidson, A.L. Maragno, G. Le Toumelin-Braizat, et al., The MCL1 inhibitor S63845 is tolerable and effective in diverse cancer models, Nature 538 (2016) 477–482.